Desalination and Water Treatment
www.deswater.com

doi: 10.5004/dwt.2019.23772

148 (2019) 188–194
April

Facile fabrication of three-dimensional and recyclable graphene oxide-melamine composites with high removal efficiency

Xiao-Ru Zhao[a], Xia Xu[a], Xin-Yu Jiang[a], Jie-Teng[b,*], Jin-Gang Yu[a,*]

[a]*College of Chemistry and Chemical Engineering, Key Laboratory of Hunan Province for Water Environment and Agriculture Product Safety, Central South University, Changsha, Hunan 410083, China, email: 2808091270@qq.com (X.-R. Zhao), 809703325@qq.com (X. Xu), jiangxinyu@csu.edu.cn (X.-Y. Jiang), Tel./Fax +86-731-88879616, email: yujg@csu.edu.cn (J.G. Yu)*

[b]*College of Materials Science and Engineering, Hunan University, Changsha, Hunan 410082, China, Tel./Fax +86-731-88821610, email: tengjie@hnu.edu.cn (J. Teng)*

Received 28 July 2018; Accepted 10 January 2019

ABSTRACT

Self-assembly of three-dimensional graphene oxide-melamine (GO-ME$_{x:y}$) composites with various GO-to-ME mass ratios (x:y) of 5:1 to 25:1 was carried out by a facile hydrothermal method. GO-ME was characterized by Fourier transform infrared (FTIR) spectroscopy and scanning electron microscopy (SEM). The adsorption properties of GO-ME toward rare earth elements (REEs), phenols and dyes in aqueous solutions were investigated. It was found that REEs could be better adsorbed onto GO-ME$_{20:1}$ with maximum adsorption capacities of 25.04, 14.08, 20.88, 19.96, 26.68 and 25.28 mg g^{-1} toward La^{3+}, Y^{3+}, Yb^{3+}, Er^{3+}, Eu^{3+} and Nd^{3+}, respectively. And GO-ME$_{15:1}$ showed relatively higher adsorption capacities of 65.77, 70.11 and 23.49 mg g^{-1} for 3-nitrophenol, p-nitrophenol and hydroquinone, respectively. Organic dyes could be preferably adsorbed by GO-ME$_{10:1}$, and its maximum adsorption capacities toward neutral red (NR) and alizarin yellow R (AYR) were 80.49 and 189.33 mg g^{-1}, respectively. In brief, GO-ME$_{x:y}$ nanocomposites were expected to be used as efficient sorbents for the adsorption removal of REEs, phenols and organic dyes.

Keywords: Graphene oxide; Melamine; Nanocomposites; Adsorption; Composite materials

---

1. Introduction

Discharged wastewater from textile industries, electroplating factories, mineral processing industries, and even sewage contains various contaminants including metal ions, phenolic and dye seriously affected the human life and the environment. For example, rare earth elements (REEs) were found in the ecological system due to the directly discharged REEs-containing wastewater, which has caused seriously negative effects to water resources, soil and human life. Both recovery and removal of REEs are urgently needed due to their high economic value as well as strong environmental pollution effects [1,2]. Phenols are widely used in medicine, pesticide, dye, photographic materials and other fields [3–5], while they are very stable and hard to degrade naturally [6–8]. Organic dyes are widely used in cosmetics, food, coatings, plastics, paper, textile and other industries, while most of organic dyes are toxic, non-biodegradable, mutagenic and/or carcinogenic, and some even cause skin irritation and human allergies [9].

Various methods including photocatalytic degradation, chemical precipitation, electrochemical degradation, ozonation and membrane filtration have been developed to remove these organic and inorganic pollutants from the contaminated wastewater [10–14]. However, these technologies are limited due to high costs, slow removal rates and secondary pollutions and so on. And adsorption has attracted great attention due to its advantages including high efficiency, low energy consumption, high removal capacity, and easy to use [15,16]. An efficient adsorption procedure usually depends on a well-developed adsorbent. Therefore, it is essential to construct novel adsorbents with high-performance.

---

*Corresponding author.

1944-3994 / 1944-3986

Graphene oxide (GO) and its derivatives/composites as efficient adsorbents have been widely studied due to their particular physical-chemical properties including large surface area and abundant active sites such as oxygen-containing functional groups (hydroxyl, carboxyl and epoxy) and π-π stacking interactions [17–21]. Additionally, the physicochemical properties of GO can be regulated by covalent modification and non-covalent coating technology, providing new opportunities for fabricating novel GO-based adsorbents [22–24]. Melamine (1,3,5-triazine-2,4,6-triamine, ME) owns three free amino groups which can covalently/non-covalently bind to other species to form different composites [25,26], providing opportunities for the fabrication of ME based adsorbents.

Three-dimensional (3D) cylindrical GO-ME composites were hydrothermally assembled through the strong hydrogen bonding interactions between GO and ME, and their adsorption capacities for various substances including rare earth elements (REEs), phenols and organic dyes in water were evaluated. The 3D GO-ME composites were expected to be used as novel, inexpensive and reusable adsorbents due to low cost of as-prepared GO, commercially available and cheap ME, and easy separation and facile recovery of the adsorbents.

2. Experiments

2.1. Materials and characterizations

Flake graphite was purchased from Qingdao Braide Graphite Co., Ltd. (Qingdao, China). Melamine was provided by Tianjin Dingshengxin Chemical Industry Co., Ltd. (Tianjin, China). Phosphoric acid (H_3PO_4, 85%), potassium permanganate ($KMnO_4$), 3-nitrophenol, p-nitrophenol and hydroquinone were obtained from Sinopharm Group Chemical Reagent Co., Ltd. (Shanghai, China). Sulfuric acid (H_2SO_4, 98%) and hydrochloric acid (HCl, 37%) were supplied by Chengdu cologne chemical Co. Ltd. (Chengdu, China). Hydrogen peroxide (H_2O_2, 30%) was purchased from Tianjin Fuqi chemical Co. Ltd. (Tianjin, China). Lanthanum chloride heptahydrate ($LaCl_3{\cdot}7H_2O$; 9.99 wt%), Yttrium chloride heptahydrate ($YCl_3{\cdot}7H_2O$; 99.90 wt%), Ytterbium chloride hexahydrate ($YbCl_3{\cdot}6H_2O$; 99.99 wt%), Erbium chloride hexahydrate ($ErCl_3{\cdot}6H_2O$; 99.90 wt%) and Neodymium chloride hexahydrate ($NdCl_3{\cdot}6H_2O$; 99.90 wt%) were bought from Aladdin Chemical Co. Ltd. (Shanghai, China). Alizarin yellow R was obtained from Xiangzhong chemical reagent development center (Chengdu, China). Neutral red was provided by Tianjin Fuchen Chemical Reagent Factory (Tianjin, China). All chemicals were used without further purification.

The surface functional groups of GO and GO-ME composite were characterized using a Shimadzu FTIR spectrophotometer (IR-prestige 21; Japan) in the wavenumber region between 4000 and 400 cm^{-1} with a resolution of 4 cm^{-1}. The morphologies and microstructures of GO and 3D GO-ME composite were characterized by scanning electron microscopy (SEM; JEOL; JSM-6360LV; Japan).

2.2. Preparation of GO dispension

GO dispersion with a concentration of 5.0 mg mL^{-1} was prepared by an improved Hummers' method [27–29]. Flake graphite (0.3 g) and 1.5 g of $KMnO_4$ were mixed together and added into a round bottom flask (100 mL). Then, a mixed acid containing 36 mL of H_2SO_4 and 4 mL H_3PO_4 (v/v = 9:1) was slowly added to the mixture to obtain a black green suspension. After it was heated to 50°C for 12 h, H_2O_2 was added into the reaction until no bubble would be produced. After that, the mixture was rinsed using HCl (1.0 mol l^{-1}) and deionized water for several times, centrifuged until the supernatant was neutral. The solid residue was dispersed in ultrapure water to obtain GO (5 mg L^{-1}) dispersion.

2.3. Preparation of 3D GO-ME composites

Various porous 3D GO-ME composites were hydrothermally fabricated. In a typical procedure, 20 mg of ME was ultrasonically dissolved in 4 mL of ultrapure water, then 20 mL of GO (5 mg L^{-1}) dispersion was added into the reaction. The mixture was sonicated for 5 min to form a homodisperse dispersion, and then transferred to a reaction vial (50.0 mL, screw cap, Teflon septa) and heated to 180°C for 4 h. After the reaction was finished, it was naturally cooled to room temperature, and porous $GO\text{-}ME_{5:1}$ composite could be obtained by freeze-drying (Fig. 1). Other porous $GO\text{-}ME_{x:y}$ composites with different GO-to-ME mass ratios (x:y = 10: 1, 15: 1, 20: 1 and 25: 1) were prepared in the same way and expressed as $GO\text{-}ME_{10:1}$, $GO\text{-}ME_{15:1}$, $GO\text{-}ME_{20:1}$ and $GO\text{-}ME_{25:1}$, respectively.

2.4. Adsorption experiments

The adsorption experiments were performed by adding a certain amount of $GO\text{-}ME_{x:y}$ composites to 20 mL of various aqueous various adsorbate-containing solutions (50 mg L^{-1}). The conical flasks containing the adsorbate and adsorbent were shaken in a constant-temperature shaker at 25°C for 5 h. The adsorbate concentrations were measured by an inductively coupled plasma-optical emission spectrometry (ICP-OES; 2X00-5000; PerkinElmer Inc., Boston, MA, USA) or a 752 UV-Vis spectrophotometer (Shanghai Jinghua Technology Instrument Co., Ltd.; Shanghai, China). The adsorption capacities of $GO\text{-}ME_{x:y}$ composites for the adsorbates could be calculated according to Eq. (1):

$$q_e = \frac{(C_0 - C_e)\times V}{m} \tag{1}$$

where q_e (mg g^{-1}) represents the adsorption capacity at equilibrium; C_0 (mg L^{-1}) is the initial concentration of contaminants solutions; C_e (mg L^{-1}) is the concentration at equilibrium; V (L) is the volume of the contaminants solutions; and m (g) is the mass of the adsorbent.

The adsorption properties of $GO\text{-}ME_{x:y}$ composites for REEs including La^{3+}, Y^{3+}, Yb^{3+}, Er^{3+}, Eu^{3+} and Nd^{3+}, phenols such as 3-nitrophenol, p-nitrophenol and hydroquinone, and organic dyes including neutral red (NR) and alizarin yellow R (AYR) were studied. To evaluate the reusability of the developed adsorbents, the adsorption of AYR and NR onto $GO\text{-}ME_{10:1}$ for 5 h at room temperature was investigated. After adsorption, the adsorbent was taken out and rinsed with ultrapure water, then used for another adsorption. The adsorption/desorption experiment was repeated three times.

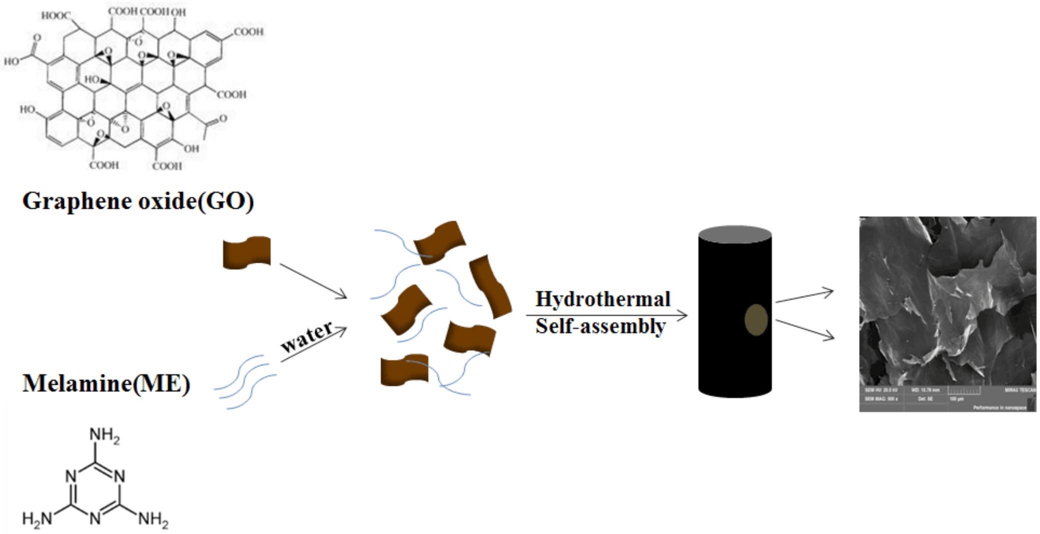

Fig. 1. Schematic diagram for hydrothermal assembly of GO-ME$_{x:y}$ composites.

3. Results and discussions

3.1. Characterization

3.1.1. IR spectroscopy

FTIR spectra of GO, ME and GO-ME$_{20:1}$ are shown in Fig. 2. The characteristic peaks at 3400 cm^{-1}, 1725 cm^{-1}, and 1617 cm^{-1} of GO could be attributed to the stretching vibration of hydroxyl group (O-H), the carboxyl group (O=C-OH) and the C=C double bonds of aromatic rings, respectively [30]. Obviously, the two characteristic peaks at 3419 cm^{-1}, 1647 cm^{-1} of ME can be assigned to the N-H and C=N stretching vibrations of melamine, respectively. By comparison, the broad peak at 1639 cm^{-1} could be attributed to the C=O stretching vibration, which shifted towards the lower wavenumber due to the possible intermolecular hydrogen bond between GO and ME.

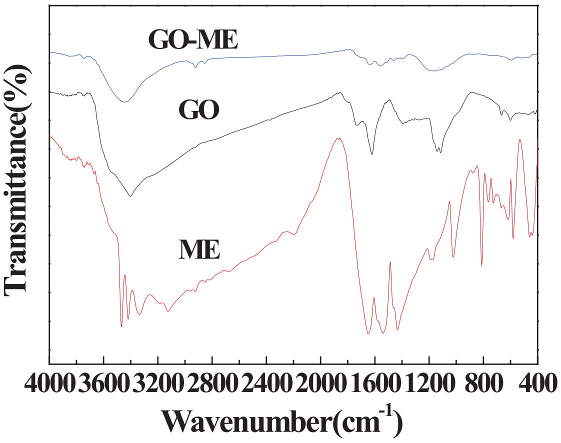

Fig. 2. FTIR spectra of GO, ME and GO-ME composite.

3.1.2. Morphological characterization

In comparison with the smooth surface of GO (Fig. 3b), GO-ME$_{20:1}$ possesses a thickened lamellar structure. Lots of folds are presented on the surface due to the assembled organic component, ME (Fig. 3c). While too much assembled ME would result in a collapsed 3D structure (Fig. 3a). And an elastic and robust structure which would facilitate the recovery is usually necessary for 3D GO-based composite [11,14].

3.2. Adsorption tests

The adsorption capacities of GO-ME$_{x:y}$ for REEs, phenols and organic dyes were evaluated. Although GO-ME$_{25:1}$ exhibited higher adsorption capacities for REEs, GO-ME$_{20:1}$ was identified as a better adsorbent because GO-ME$_{25:1}$ was easy to be collapsed and difficult to recycle. GO-ME$_{20:1}$ showed adsorption uptakes of 25.04, 14.08, 20.88, 19.96, 26.68 and 25.28 mg g^{-1} for La^{3+}, Y^{3+}, Yb^{3+}, Er^{3+}, Eu^{3+} and Nd^{3+}, respectively (Fig. 4a). Due to the small complexation constant of REEs and N-containing compounds, the adsorption capacities of GO-ME$_{20:1}$ composite for REEs were relatively low [31]. GO-ME$_{20:1}$ composite showed lower adsorption capacity for Y^{3+}, indicating the complexation constant of Y^{3+} and N-containing compounds was the smallest. Phenols could be well adsorbed on GO-ME$_{15:1}$, and its adsorption capacities for 3-nitrophenol, p-nitrophenol and hydroquinone were 65.77, 70.11 and 23.49 mg g^{-1}, respectively (Fig. 4b). The acidities of the phenols are p-nitrophenol > 3-nitrophenol >> hydroquinone, the low adsorption capacity of GO-ME$_{15:1}$ composite for hydroquinone could be observed due to the relatively weaker acid-base interactions. That is to say, the interactions of –NH$_2$ groups on GO-ME$_{15:1}$ composite with these phenols contributed a lot to the efficient adsorption. GO-ME$_{10:1}$ showed relatively higher adsorption capacities of 80.49 and 189.33 mg g^{-1} for AYR and NR, respectively (Fig. 4c). The results indicated that the adsorption efficiencies of GO-ME$_{x:y}$ could be regulated by changing GO-to-ME mass ratios.

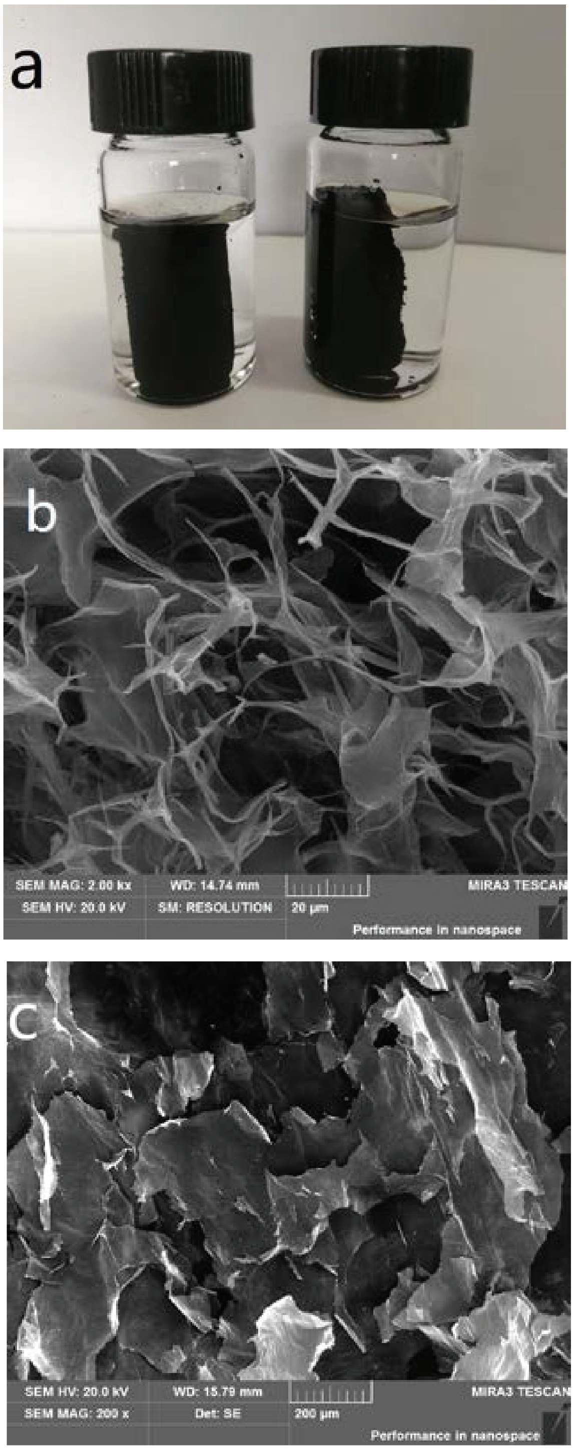

Fig. 3. A comparison of morphologies of the samples: (a) Photographs of GO-ME$_{5:1}$ (left) and GO-ME$_{25:1}$; (b) SEM images of GO; (c) SEM images of GO-ME$_{20:1}$.

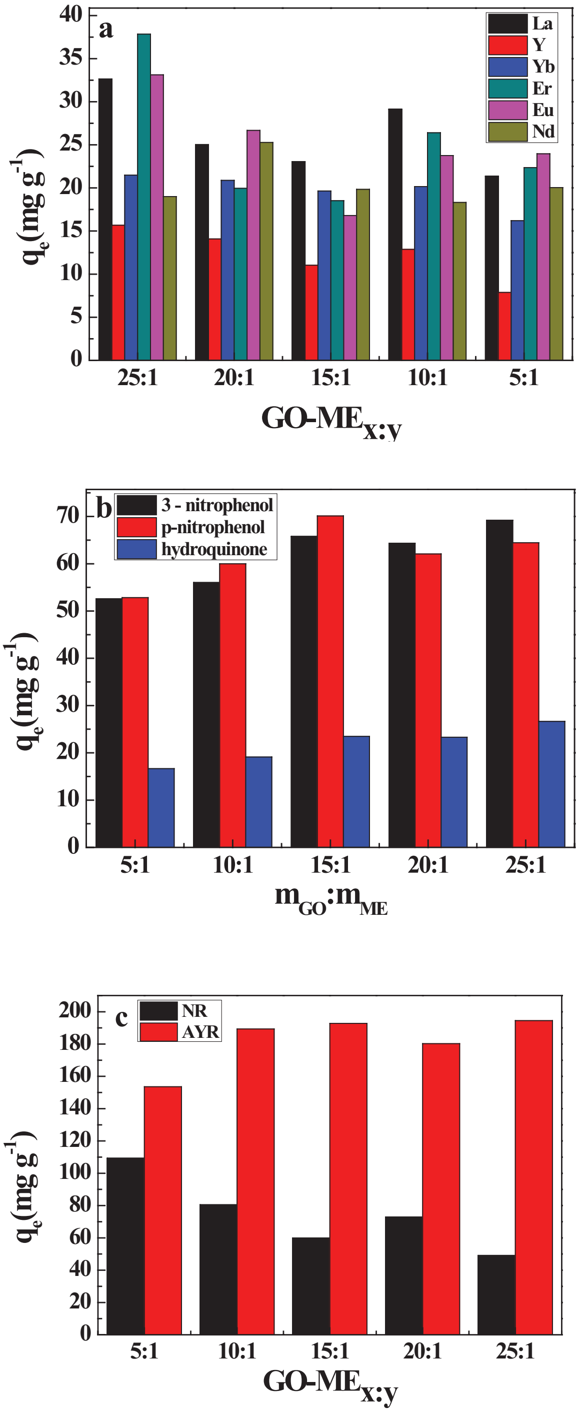

Fig. 4. The adsorption performance of GO-ME$_{x:y}$ composites for various adsorbates: (a) REEs; (b) Phenols; (c) Organic dyes.

3.3. Repeated adsorption/desorption experiments

Repeated adsorption/desorption experiments were performed. As it can be seen from Fig. 5, the removal rates of GO-ME$_{10:1}$ for AYR and NR were almost 100% even after 3 cycles of adsorption/desorption procedures, which was better than previously reported GO-based adsorbents [23,32], indicating the fabricated 3D GO-ME$_{x:y}$ could be used as efficient and reusable adsorbents.

Reusability is a crucial factor in the practical application of a newly-developed adsorbent. For this reason, 3 cycles of adsorption/desorption experiments were carried out for GO-ME $_{20:1}$ composite toward two organic dyes, NR and

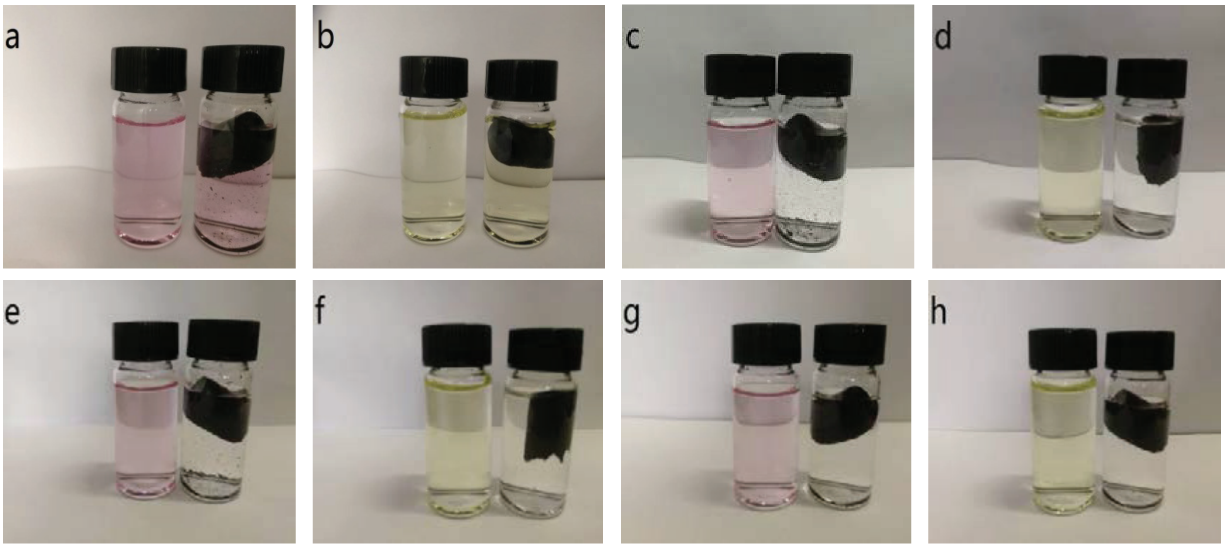

Fig. 5. Repeated adsorption/desorption experiments for GO-ME$_{10:1}$ (Red: NR; Yellow: AYR): (a-b) before adsorption; (c-d) first adsorption; (e-f) second adsorption; (g-h) third adsorption.

AYR, with an initial concentration of 10 ppm, and ultrapure water was used as the desorption reagent. It is obvious that GO-ME$_{20:1}$ composite still retained removal efficiencies of ~90% for the adsorption/desorption of NR or AYR (Fig. 6).

3.4. A comparison with previously reported adsorbents

As shown in Table 1, the removal efficiencies of GO-ME$_{10:1}$ composite for organic dyes are compared with some previously reported adsorbents. Obviously, GO-ME$_{10:1}$ composite possessed relatively higher removal efficiencies than those of magnetic metal-organic framework (MOF) [33], Fe@C magnetic nanocapsules [34], acrylic acid-acrylonitrile-N-isopropylacrylamide (AA-AN-N-IPAA) polymeric gel [35] and pentaerythritol modified multi-walled carbon nanotubes (ox-MWCNT-PER) [36]. Although the nanoporous polyethylene imine (PEI) functionalized silica (Si-PEI) possessed higher adsorption capacity for AYR [37], GO-ME composites showed better reusability. In addition, the procedure for the fabrication of GO-ME composites was relatively more facile and time-saving. Therefore, the practical application of the developed GO-ME composites for the removal/enrichment of organic/inorganic substances from water is greatly anticipated.

4. Conclusions

GO-ME$_{x:y}$ nanocomposites with different GO-to-ME mass ratios were hydrothermally fabricated and characterized. The removal efficiencies of GO-ME$_{x:y}$ composites for REEs, phenols and organic dyes in water were investigated. It was found that the adsorption efficiencies of GO-ME$_{x:y}$ could be regulated by changing GO-to-ME mass ratios. Moreover, 3D GO-ME$_{x:y}$ could be easily recycled and possessed higher removal efficiencies even after 5 cycles of adsorption/desorption procedures. It can be expected that GO-ME$_{x:y}$ composites may be used as efficient and reusable adsorbents.

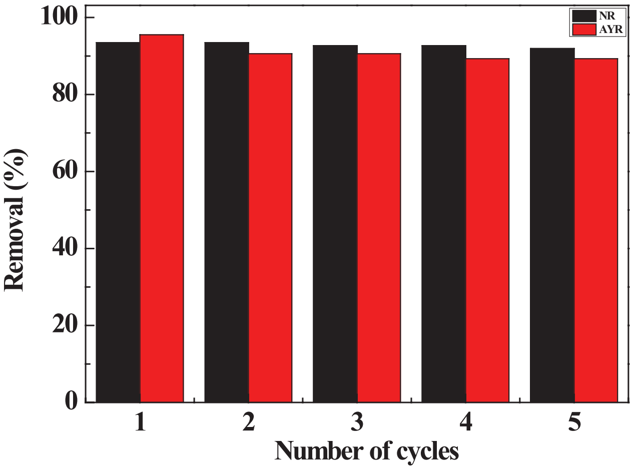

Fig. 6. The reusability of GO-ME$_{10:1}$ composite for adsorption/desorption of NR and AYR.

Table 1
A comparison of GO-ME$_{10:1}$ for organic dyes with some previously reported adsorbents

Adsorbent	Adsorption capacity for dyes (mg/g)	Ref.
MOF	30 mg/g for methylene blue (MB)	[33]
AA-AN-N-IPAA	2.79 mg/g for MB	[35]
Fe@C	44.5 mg/g for MB	[34]
ox-MWCNT-PER	45.39 mg/g for AYR	[36]
Si-PEI	400 mg/g for AYR	[37]
GO-ME$_{10:1}$	80.49 and 189.33 mg g^{-1} for AYR and NR, respectively	This work

Acknowledgment

We greatly appreciate the financial supports from National Natural Science Foundation of China (Nos. 51674292, 21471163 and 51574118), Provincial Natural Science Foundation of Hunan (No. 2016JJ1023) and Hunan Provincial Science and Technology Plan Project, China (No. 2018TP1003).

References

[1] R.A. Schmitt, R.H. Smith, J.E. Lasch, A.W. Mosen, D.A. Olehy, J. Vasilevskis, Abundances of the fourteen rare-earth elements, scandium, and yttrium in meteoritic and terrestrial matter, Geochim. Cosmochim. Acta, 27 (1963) 577–622.

[2] W. Gwenzi, L. Mangori, C. Danha, N. Chaukura, N. Dunjana, E. Sanganyado, Sources, behaviour, and environmental and human health risks of high-technology rare earth elements as emerging contaminants, Sci. Total Environ., 636 (2018) 299–313.

[3] M. Peng, X. Tang, Y. Zhou, Fast phase transfer of graphene oxide from water to triglycidyl para-aminophenol for epoxy composites with superior nanosheet dispersion, Polymer, 93 (2016) 1–8.

[4] H. Bahrami, H. Salehabadi, Experimental and theoretical investigation of para-aminophenol ionization in corona discharge, J. Mol. Struct., 1083 (2015) 330–335.

[5] T. Komatsu, T. Hirose, Gas phase synthesis of para-aminophenol from nitrobenzene on Pt/zeolite catalysts, Appl. Catal. A-Gen., 276 (2004) 95–102.

[6] S.L. Chen, Z.P. Xu, Q. Zhang, G.Q.M. Lu, Z.P. Hao, S.M. Liu, Studies on adsorption of phenol and 4-nitrophenol on MgAl-mixed oxide derived from MgAl-layered double hydroxide, Sep. Purif. Technol., 67 (2009) 194–200.

[7] J. Zou, X.Q. Chen, G.Q. Zhao, X.Y. Jiang, F.P. Jiao, J.G. Yu, A novel electrochemical chiral interface based on the synergistic effect of polysaccharides for the recognition of tyrosine enantiomers, Talanta, 195 (2019) 628–637.

[8] J. Yang, B. Yue, J. Teng, X. Xu, X. Zhao, X. Jiang, J. Yu, F. Zhou, Aqueous metal ions adsorption by poly(ethylene glycol) modified graphene oxide: surface area and surface chemistry effects, Desal. Water Treat., 138 (2019) 147–158.

[9] M. Ghaedi, A. Hassanzadeh, S.N. Kokhdan, Multiwalled carbon nanotubes as adsorbents for the kinetic and equilibrium study of the removal of alizarin red S and morin, J. Chem. Eng. Data, 56 (2011) 2511–2520.

[10] Z. Wu, H. Zhong, X. Yuan, H. Wang, L. Wang, X. Chen, G. Zeng, Y. Wu, Adsorptive removal of methylene blue by rhamnolipid-functionalized graphene oxide from wastewater, Water Res., 67 (2014) 330–344.

[11] L. Zhu, M. Gao, C.K.N. Peh, X. Wang, G.W. Ho, Carbon sponges: Self-contained monolithic carbon sponges for solar-driven interfacial water evaporation distillation and electricity generation, Adv. Energy Mater., 8 (2018) 1870074.

[12] S.W.L. Ng, G. Yilmaz, W.L. Ong, G.W. Ho, One-step activation towards spontaneous etching of hollow and hierarchical porous carbon nanospheres for enhanced pollutant adsorption and energy storage, Appl. Catal. B-Environ., 220 (2018) 533–541.

[13] W.L. Ong, J.H.M. Wong, S.W.L. Ng, H.R. Tan, Y.F. Lim, G.W. Ho, Simultaneous activation–exfoliation–reassembly to form layered carbon with hierarchical pores, Chem. Cat. Chem., 9 (2017) 2488–2495.

[14] L. Zhu, C. Fu Tan, M. Gao, G.W. Ho, Design of a metal oxide–organic framework (MoOF) foam microreactor: Solar-induced direct pollutant degradation and hydrogen generation, Adv. Mater., 27 (2015) 7713–7719.

[15] W. Zhan, S. Yu, L. Gao, F. Wang, X. Fu, G. Sui, X. Yang, Bioinspired assembly of carbon nanotube into graphene aerogel with "cabbage like" hierarchical porous structure for highly efficient organic pollutants cleanup, ACS Appl. Mater. Interf., 10 (2018) 1093–1103.

[16] P. Sharma, N. Hussain, D.J. Borah, M.R. Das, Kinetics and adsorption behavior of the methyl blue at the graphene oxide/reduced graphene oxide nanosheet–water interface: a comparative study, J. Chem. Eng. Data, 58 (2013) 3477–3488.

[17] C.C. Dong, J. Lu, B.C. Qiu, B. Shen, M.Y. Xing, J.L. Zhang, Developing stretchable and graphene-oxide-based hydrogel for the removal of organic pollutants and metal ions, Appl. Catal. B-Environ., 222 (2018) 146–156.

[18] J.L. Xiao, W.Y. Lv, Z. Xie, Y.Q. Tan, Y.H. Song, Q. Zheng, Environmentally friendly reduced graphene oxide as a broad-spectrum adsorbent for anionic and cationic dyes via pi-pi interactions, J. Mater. Chem. A, 4 (2016) 12126–12135.

[19] I. Duru, D. Ege, A.R. Kamali, Graphene oxides for removal of heavy and precious metals from wastewater, J. Mater. Sci., 51 (2016) 6097–6116.

[20] J. Zou, G. Zhao, J. Teng, Q. Liu, X. Jiang, F. Jiao, J. Yu, Highly sensitive detection of bisphenol A in real water samples based on in-situ assembled graphene nanoplatelets and gold nanoparticles composite, Microchem. J., 145 (2019) 693–702.

[21] J. Zou, L. Huang, X. Jiang, F. Jiao, J. Yu, Electrochemical behaviors and determination of rifampicin on graphene nanoplatelets modified glassy carbon electrode in sulfuric acid solution, Desal. Water Treat., 120 (2018) 272–281.

[22] Z.H. Sheng, L. Shao, J.J. Chen, W.J. Bao, F.B. Wang, X.H. Xia, Catalyst-free synthesis of nitrogen-doped graphene via thermal annealing graphite oxide with melamine and its excellent electrocatalysis, ACS Nano, 5 (2011) 4350–4358.

[23] Z.N. Huang, J. Zou, J. Teng, Q. Liu, M.M. Yuan, F.P. Jiao, X.Y. Jiang, J.G. Yu, A novel electrochemical sensor based on self-assembled platinum nanochains - Multi-walled carbon nanotubes-graphene nanoparticles composite for simultaneous determination of dopamine and ascorbic acid, Ecotox. Environ. Safe., 172 (2019) 167–175.

[24] X. Xu, J. Zou, J. Teng, Q. Liu, X.Y. Jiang, F.P. Jiao, J.G. Yu, X.Q. Chen, Novel high-gluten flour physically cross-linked graphene oxide composites: Hydrothermal fabrication and adsorption properties for rare earth ions, Ecotox. Environ. Safe., 166 (2018) 1–10.

[25] N. Yusof, S. Rahman, M. Hussein, N. Ibrahim, Preparation and characterization of molecularly imprinted polymer as SPE sorbent for melamine isolation, Polymers, 5 (2013) 1215–1228.

[26] A. Hayashi, H. Nakayama, M. Tsuhako, Intercalation of melamine into layered zirconium phosphates and their adsorption properties of formaldehyde in gas and solution phase, Solid State Sci., 11 (2009) 1007–1015.

[27] C. Wu, Q.Y. Cheng, S.Q. Sun, B.H. Han, Templated patterning of graphene oxide using self-assembled monolayers, Carbon, 50 (2012) 1083–1089.

[28] J.J. Xu, K. Wang, S.Z. Zu, B.H. Han, Z.X. Wei, Hierarchical nanocomposites of polyaniline nanowire arrays on graphene oxide sheets with synergistic effect for energy storage, ACS Nano, 4 (2010) 5019–5026.

[29] X. Zeng, J. Yu, D. Fu, H. Zhang, J. Teng, Wear characteristics of hybrid aluminum-matrix composites reinforced with well-dispersed reduced graphene oxide nanosheets and silicon carbide particulates, Vacuum, 155 (2018) 364–375.

[30] X. Zeng, J. Teng, J.G. Yu, A.S. Tan, D.F. Fu, H. Zhang, Fabrication of homogeneously dispersed graphene/Al composites by solution mixing and powder metallurgy, Int. J. Miner. Metall. Mater., 25 (2018) 102–109.

[31] H. Gao, D. Chen, J. Wu, G. Xu, Determination of stability constants of mixed ligand complexes of rare earths by method of two-phase titrations, Chem. J. Chin. Univ.-Chin., 2 (1981) 417–422.

[32] B. Yue, L. Yu, F. Jiao, X. Jiang, J. Yu, The fabrication of pentaerythritol pillared graphene oxide composite and its adsorption performance towards metal ions from aqueous solutions, Desal. Water Treat., 102 (2018) 124–133.

[33] X.L. Zhao, S.L. Liu, Z. Tang, H.Y. Niu, Y.Q. Cai, W. Meng, F.C. Wu, J.P. Giesy, Synthesis of magnetic metal-organic framework (MOF) for efficient removal of organic dyes from water, Sci. Rep., 5 (2015).

[34] R.R. Li, J.Y. Yu, A. Shah, X.L. Dong, X.N. Li, H.T. Yu, X. Quan, Y. Jung, Novel in situ synthesized Fe@C magnetic nanocapsules used as adsorbent for removal of organic dyes and its recycling, Nano, 11 (2016).

[35] M.A. Malana, S. Parveen, R.B. Qureshi, Adsorptive removal of organic dyes from aqueous solutions using acrylic acid-acrylonitrile-N-isopropylacrylamide polymeric gels as adsorbents: linear and non linear isotherms, Desal. Water Treat., 57 (2016) 22543–22550.

[36] J. Yang, X. Jiang, F. Jiao, J. Yu, The oxygen-rich pentaerythritol modified multi-walled carbon nanotube as an efficient adsorbent for aqueous removal of alizarin yellow R and alizarin red S, Appl. Surf. Sci., 436 (2018) 198–206.

[37] L. Adlnasab, M. Shabanian, M. Ezoddin, A. Maghsodi, Amine rich functionalized mesoporous silica for the effective removal of alizarin yellow and phenol red dyes from waste waters based on response surface methodology, Mater. Sci. Eng. B-Solid State Mater. Adv. Technol., 226 (2017) 188–198.